

AD-A280 465

ATION PAGE

Form Approved
OMB No. 0704-0188

①

to average 1 hour per response, including the time for reviewing instructions, searching existing data sources, gathering the collection of information. Send comments regarding this burden estimate or any other aspect of this form to Washington Headquarters Services, Directorate for Information Operations and Reports, 1215 Jefferson Avenue, Management and Budget, Paperwork Reduction Project (0704-0188), Washington, DC 20503.

1. AGENCY USE ONLY (Leave blank)		2. REPORT DATE		3. REPORT TYPE AND DATES COVERED FINAL REPORT - 1 May 89 - 30 Apr 94	
4. TITLE AND SUBTITLE Basic Studies in Plasma Wave Interactions				5. FUNDING NUMBERS 61102F 2301/ES	
6. AUTHOR(S) J.E. Scharer					
7. PERFORMING ORGANIZATION NAME(S) AND ADDRESS(ES) Department of Electrical & Computer Engineering University of Wisconsin Madison, WI 53706				8. PERFORMING ORGANIZATION REPORT NUMBER AFOSR-TR- 94 0368	
9. SPONSORING/MONITORING AGENCY NAME(S) AND ADDRESS(ES) AFOSR/NE 110 Duncan Avenue Suite B115 Bolling AFB DC 20332-0001				10. SPONSORING/MONITORING AGENCY REPORT NUMBER AFOSR-89-0353	
11. SUPPLEMENTARY NOTES DTIC QUALITY INSPECTED 2					
12a. DISTRIBUTION/AVAILABILITY STATEMENT APPROVED FOR PUBLIC RELEASE: DISTRIBUTION UNLIMITED				12b. DISTRIBUTION CODE	
13. ABSTRACT (Maximum 200 words) Research on microwave propagation, reflection, absorption and backscatter in XUV excimer laser (193 nm) and microwave (2.45 GHz) produced plasmas has been carried out. Our research on high density, low temperature ($n_e = 5 \times 10^{13}/\text{cm}^3$, 1 eV) laser-created plasma and broadband (1-3 GHz) microwave transmission, absorption and backscatter between two antennas in a plasma are described. Research on the creation of a laser produced sheet beam plasma for either a low loss, rapidly scanable agile microwave mirror reflector (10 GHz) or a diffuse, lossy absorber is being carried out. Measurements and theoretical analysis of these topics are described. We also discuss our collaborations with other research groups and our theoretical and computational research to support and interpret the experimental observations.					
14. SUBJECT TERMS				15. NUMBER OF PAGES	
				16. PRICE CODE	
17. SECURITY CLASSIFICATION OF REPORT UNCLASSIFIED		18. SECURITY CLASSIFICATION OF THIS PAGE UNCLASSIFIED		19. SECURITY CLASSIFICATION OF ABSTRACT UNCLASSIFIED	
				20. LIMITATION OF ABSTRACT UNCLASSIFIED	

94-18979



6

20

6

54

AEDSR-TR- 94 0368

**Final Technical Report
May 1, 1991 - April 30, 1994**

**Approved for public release;
distribution unlimited.**

Basic Studies in Plasma/Wave Interactions

**J.E. Scharer, Principal Investigator
Department of Electrical and Computer Engineering
University of Wisconsin
Madison, WI 53706**

AFOSR Grant 89-0353 B

May, 1994

**Approved for public release;
distribution unlimited.**

Final Report
Basic Research on Plasma-Wave Interactions
University of Wisconsin
For AFOSR Grant No AFOSR-89-0353
May, 1994

Abstract

Research on microwave propagation, reflection, absorption and backscatter in XUV excimer laser (193 nm) and microwave (2.45 GHz) produced plasmas has been carried out. Our research on high density, low temperature ($n_e = 5 \times 10^{13}/\text{cm}^3$, 1 eV) laser-created plasma and broadband (1-3 GHz) microwave transmission, absorption and backscatter between two antennas in a plasma are described. Research on the creation of a laser produced sheet beam plasma for either a low loss, rapidly scanable agile microwave mirror reflector (10 GHz) or a diffuse, lossy absorber is being carried out. Measurements and theoretical analysis of these topics are described. We also discuss our collaborations with other research groups and our theoretical and computational research to support and interpret the experimental observations.

I. Introduction

The experimental and theoretical research carried out in the past three years involves 1) creation of plasmas to provide an agile mirror for airborne or shipboard scanning of microwave and millimeter wave systems and 2) creation of collisional absorbing plasmas to reduce 1-10 GHz radar transmission and return from objects located in the earth's atmosphere. The research is also relevant to the reduction of radar cross section and protection of systems from high power transmission microwave jamming meant to disable communications. The research topics addressed include: 1) XUV (extreme ultraviolet $\lambda = 193$ nm) excimer laser creation of agile mirror microwave reflecting and absorbing plasma layers. 2) Microwave cross section and backscatter measurements from antennas in a microwave produced plasma. 3) Associated theoretical and computational modelling and data analysis for mirror reflection, absorption and backscatter as well as plasma sources to elucidate experimental observations and to predict future experimental results.

We have completed construction of a sheet beam excimer laser and plasma vacuum facility to study microwave reflection and absorption from a sheet beam produced plasma. Cylindrical lenses are used to produce a 1.4 mm x 110 mm laser beam ($\lambda = 193$ nm, 15 mJ, $\tau = 17$ ns and 200 Hz rep rate) for ionization of an organic gas ($n_e \geq 1 \times 10^{13}/\text{cm}^3$) to produce a microwave agile mirror reflector. By adjusting the optical system to increase the plasma thickness to 35 mm at lower density ($n_e = 10^{11} - 10^{12}/\text{cm}^3$) and raising the gas neutral pressure to make it more collisional, an absorbing layer with low reflections can be created by optical means.

We have published¹ our results on broadband microwave absorption and backscatter measurements utilizing a modulated scatterer and network analyzer techniques which describe the two-port properties of two microwave antennas in a plasma. We have also benefited from our interactions and visits with Drs. Stadler, Eckstrom and Vidmar of the Stanford Research Institute on the low ionization energies from organic gases and their use for microwave absorption. J.E. Scharer visited their laboratory to discuss their experiment and objectives before we carried out our XUV excimer laser plasma experiment. We have carried out and have published² measurements of XUV laser attenuation, plasma creation, photon absorption cross section, recombination and microwave reflection from the plasma. We are also collaborating with Drs. Smithe and Goplen of the Mission Research Corporation in Alexandria, Virginia regarding the use of the MAGIC code for modelling and analysis of two and three dimensional descriptions of microwave radiation from a helix and test antenna backscatter in a plasma column. We have examined XUV laser produced plasmas to describe the plasma uniformity and its influence on microwave reflections.

Our current research group consists of Professor J. Scharer and scientists Dr. N. Lam and Dr. W. Shen. Graduate students Brian Chapman, Yannikis Mouzouris and Brad Porter are completing their M.S. theses and are continuing towards the Ph.D. degree.

II. Progress on Basic Research on Plasma-Wave Interactions

A. Collisional Plasma Production by Ultraviolet Ionization of a Low Ionization Organic Gas

For	
RI	<input checked="" type="checkbox"/>
d	<input type="checkbox"/>
Don	<input type="checkbox"/>
Availability Codes	
Dist	Avail and/or Special
A-1	

A.1 Measurement of 193 nm Absorption and Recombination in TMAE

We have carried out initial excimer laser and flashtube experiments to explore plasma production by ultraviolet radiation. We plan to produce plasmas ($n_e \approx 10^{12}/\text{cm}^3$) with either a high density neutral gas background ($p_n \approx 200$ mTorr), producing collisional microwave absorption with negligible reflections as well as a high density ($n_e \approx 1 \times 10^{13}/\text{cm}^3$, low collisional ($\nu/\omega_p \approx 10^{-4}$) sharp boundary reflecting mirror.

The ionization is produced by the photoelectric effect from ultraviolet radiation, a much different mechanism than the impact ionization utilized in our electron cyclotron resonance plasma sources. Photoionization occurs in one step, since the incident photon has an energy above the ionization energy. Vidmar³, and Stadler et al.⁴ have carried out previous work on collisional plasmas to absorb microwave power. With electron cyclotron sources, the ionization is a multi-step process. Electrons are accelerated near resonance and gain enough energy to raise a neutral atom to an excited state or impact ionize the neutral atom.

In these experiments we have used ultraviolet radiation produced by two sources: a commercial flashtube filled with Xenon, and also the radiation of an excimer laser filled with an Argon-Fluorine gas mixture. The flashtube produced up to 100 mJ of wideband radiation with wavelengths greater than about 180 nm. The laser operates at 193 nm, producing up to 20 mJ at this wavelength.

The experiments were done on an ionization test stand that is shown in Fig. 1. The vacuum chamber is a glass cross shaped tube which is 15 cm in diameter, with overall dimensions of 50 cm by 50 cm. The chamber is pumped by a diffusion pump, backed by a mechanical forepump. The neutral pressure is measured by three gauges, a mechanical Bourdon gauge that operated in the range of 1 Torr to atmospheric pressure, a thermocouple gauge that operated from 1 m Torr to 1 Torr and an ionization gauge that operates from 1 n Torr to 1 m Torr. We have explored plasma production over a narrow pressure range and plan to do so over a much wider range.

Two Suprasil windows, each 3/16" thick and 2" diameter, are mounted in both ends of the test stand allowing the laser beam to pass. These windows are

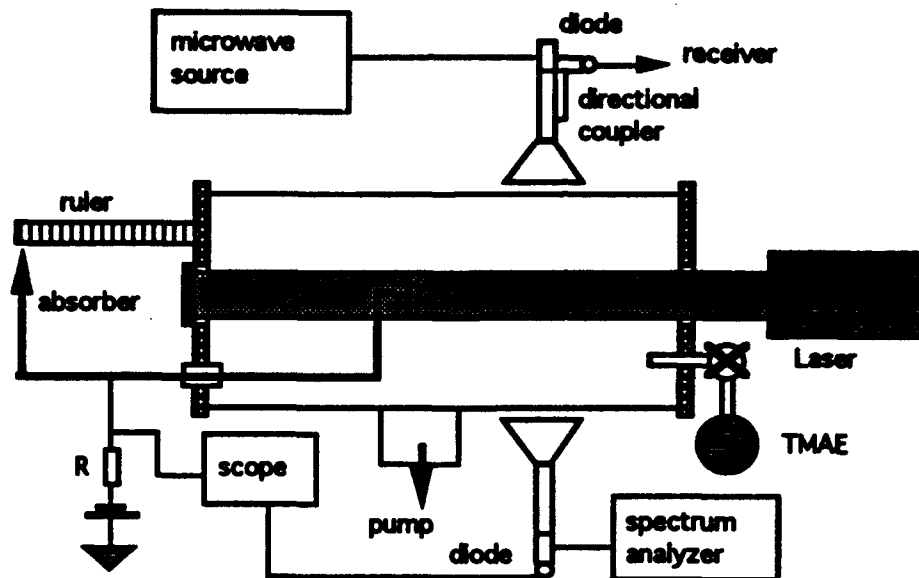


Fig. 1. Excimer laser plasma ionization facility

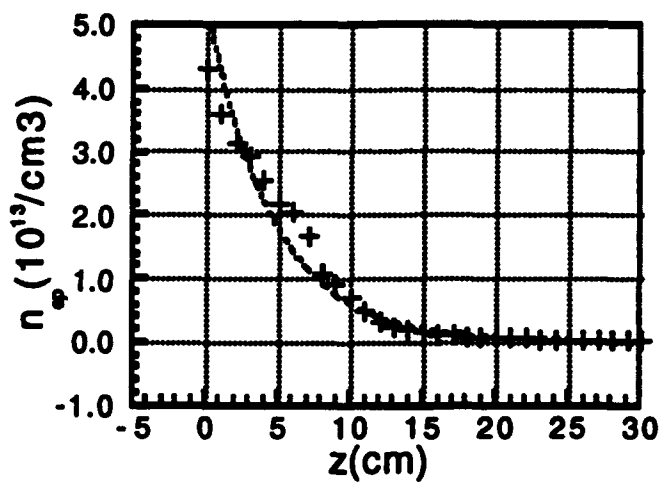


Fig. 2. Plasma density produced due to 193 nm laser attenuation in a high neutral pressure TMAE gas ($p = 500$ mTorr).

purified quartz, SiO₂, and pass 90% of the radiation with wavelengths longer than 170 nm. The plasma density produced by a flashtube mounted outside the chamber has also been measured by a Langmuir probe and by a microwave interferometer operating at a frequency of 8.9 GHz.

The gas mixture used for the experiments was TMAE, tetrakis (dimethylamino) - ethylene in argon or as pure TMAE. TMAE has an ionization potential of 5.36 ± 0.02 eV, corresponding to a threshold wavelength of 231.3 nm. The laser wavelength of 193 nm produces a photon with energy 6.42 eV, so that single stage photoionization occurs with an excited electron of 1.06 eV kinetic energy. A maximum plasma density of $n = 5 \times 10^{13} \text{ cm}^{-3}$ was produced by 193 nm laser irradiation, and a maximum $n = 2 \times 10^{11} \text{ cm}^{-3}$ was obtained by the flashlamp. These experiments were encouraging and will be repeated at higher ultraviolet power levels and with different low ionization and noble "nurse" gas concentrations in the proposed research. We have measured (see Fig. 2) and have published the 193 nm laser attenuation results in a pure TMAE plasma.² Our experiments show that at lower TMAE pressures ($p_0 = 50$ mTorr) uniform plasma densities of $n_e = 2 \times 10^{13} / \text{cm}^3$ can be produced over the whole 500 mm length of the vacuum chamber. The results provide a measurement of the 193 nm ionization cross section and recombination coefficient in TMAE. The laser and Langmuir probe measurement methods are more direct than and superior to previous research on XUV ionization of TMAE.

We have developed a one photon ionization model to describe the laser ionization. It is well known that the impact of a photon on a molecule can cause ionization, if the photon energy $E_0 = h\nu$ is greater than the ionization threshold of the molecule. We consider a photon flux propagating through a molecular gas, assuming that the photoionization is the main absorption process, and omitting the absorption of photons by TMAE ions. The equation describing the photon flux propagation and absorption is derived to be

$$\frac{\partial \Gamma}{\partial t} = -\frac{c}{n} \frac{\partial \Gamma}{\partial z} - \frac{c}{n} \Gamma (n_m - n_e) \sigma_a \quad (1)$$

where Γ is the photon flux; and n_e and n_m are electron density and neutral molecular density; σ_a is the photon absorption cross-section, c is the speed of light in the vacuum, and n is the index of refraction, in our experiment $n=1$, since the laser frequency is much higher than the plasma frequency.

The ionization and electron loss processes can be described by

$$\frac{\partial n_e}{\partial t} = \Gamma(n_m - n_e)\sigma_i + \alpha_d \frac{\partial^2 n_e}{\partial z^2} - \alpha_r n_e^2 - \alpha_a n_e \quad (2)$$

where σ_i is the ionization cross-section; α_d , α_r , and α_a are the plasma diffusion coefficient, electron-ion recombination coefficient, and electron attachment frequency to neutral molecules, respectively. The solution of Eqns. (1) and (2) yields the spatial and temporal evolution of electron density and photon flux, which are often of interest in pulsed photon ionization experiments and applications.

We have measured the (193 nm) photon absorption cross-section and recombination coefficient for the TMAE molecule and carried out a microwave scattering experiment in the TMAE plasma. Equations (1) and (2) are general descriptions of photon flux in a gas medium where the molecules' ionization potential is less than the photon energy. If the photon flux is a short pulse of width τ , during that time the electron density will not be affected by diffusion, or recombination, or attachment processes and the percentage of ionization will remain small i.e. $n_e \ll n_m$; then Eqns. (1) and (2) can be simplified to

$$\frac{\partial \Gamma}{\partial z} = -\Gamma n_m \sigma_a \quad (5)$$

where $n_m \sigma_a = k_a$ is the absorption coefficient, and

$$n_e = \Gamma n_m \sigma_a \tau \quad (6)$$

The solution of (5) is

$$n_e(Z) = n_e(0) \exp(-n_m \sigma_a Z) \quad (7)$$

where $n_e(0) = \Gamma(0) n_m \sigma_i \tau$. The absorption cross-section of TMAE vapor can then be determined after the measurement of the electron density spatial profile along the direction of laser propagation.

The plasma decay process can be described by Eq. (2) by setting $\Gamma = 0$

$$\frac{\partial n_e}{\partial t} = \alpha_d \frac{\partial^2 n_e}{\partial z^2} - \alpha_r n_e^2 - \alpha_a n_e \quad (10)$$

By considering the ambipolar diffusion time in TMAE, we determined that diffusion inside the laser beam can be neglected for time scales shorter than 1 ms. We estimated the effective attachment rate using available data on electron attachment to oxygen and determined that the decay time constant is of the order of

10 ms. So the initial decay of electron density is dominated by electron-ion recombination, and it obeys the well-known simple equation

$$n(t) = \frac{n_0}{n_0 \alpha_r t + 1} \quad (11)$$

where n_0 is the initial electron density.

The initial electron decay density is measured by means of a Langmuir probe. We plotted the inverse of electron density versus time. The good fit of the experimental data to a linear function shows that the decay process is, indeed, recombination. The recombination coefficient is determined to be $5.4 \pm 0.5 \times 10^{-6} \text{ cm}^3/\text{s}$.

The microwave reflection experimental setup is shown in Fig. 1. The peak electron density in the region in front of the antenna was measured by a Langmuir probe to be $3 \times 10^{13} \text{ cm}^{-3}$ at a pressure of 250 mTorr. The reflected wave is measured by a diode detector through a directional coupler, which is shown in Fig. 1. The peak reflected power is 0.33 mW. For comparison, the 8.7 GHz microwave signal reflected from a copper x-band waveguide (25 mm x 13 mm) placed at the same position as the plasma column is measured to be 0.45 mW. The result demonstrates that reflection due to the TMAE plasma can be very effective. In the future we plan to produce a sheet ultraviolet laser beam to create a high density gradient TMAE plasma sheet with a width an order of magnitude larger than the wavelength of the microwaves. The plasma sheet should efficiently reflect the microwaves. If the XUV laser beam is optically rotated, a rotating mirror reflector as a variant of the agile mirror concept⁶ is produced which would be attractive for radar scanning applications at microwave or millimeter wavelengths.

A.2. Recent Progress on an XUV Laser Created Agile Mirror

a) Experimental set up

We have designed and fabricated a new system to carry out detailed investigation of laser-induced plasma including beam profile modification scheme, and to investigate wave-plasma interactions in such a system. The goal of the work

is to study the application of using an XUV laser produced plasma with an optically determined profile to either reflect or absorb microwaves.

The core of the new system is a set of cylindrical lenses which are specially coated to have high transparency (98%) at 193 nm. This lens system (Fig. 3) allows us to optically transform the output laser beam profile to obtain desirable plasma dimensions. The first two lenses compress the input beam (initially 2.2 cm x 0.7 cm) vertically by a factor of 5, and the last two lenses expand the beam horizontally by a factor of 5. The output laser beam (11 cm x 1.4 mm) is then passed through TMAE gas to generate a plasma sheet via photo-ionization process. A useful feature of the configuration in Fig. 3 is that the same system can also be used to produce thick (3 - 5 cm) and dense plasma layer for the wave absorption studies with minimal modification. By simply switching the first two lenses, the output plasma beam becomes 11 cm x 3.5 cm.

We have also developed an XUV optical detection system utilizing an XUV sensitive photo-diodes to monitor the laser power distribution. This allows us to have a better understanding of photo-ionization process in TMAE.

We have also designed and constructed a new gas tank to host the XUV transparent Suprasil lenses in a nitrogen environment. This is to reduce the laser power attenuation (5 dB/m) due to O₂ absorption. A 193 nm XUV laser is strongly absorbed when O₂ is presented. Figure 4 (Photo) shows the new Nitrogen tank with lenses enclosed. Figure 5 shows the overall layout with the planned microwave reflection system installed.

b) Experimental results

The TMAE plasma generated with excimer laser has the life time of few to few-hundred micro-seconds depending on the initial filling TMAE pressure. This is much longer than the beam duration time of < 20 ns.

Initial 2-D plasma profiles have been measured with single tip Langmuir probes. We have recently made more sophisticated triple probes⁶ to obtain temperature and density simultaneously. The measurement yields (Fig. 6) a peak plasma density of $1.2 \times 10^{13} \text{ cm}^{-3}$ near the beam entrance when the initial neutral

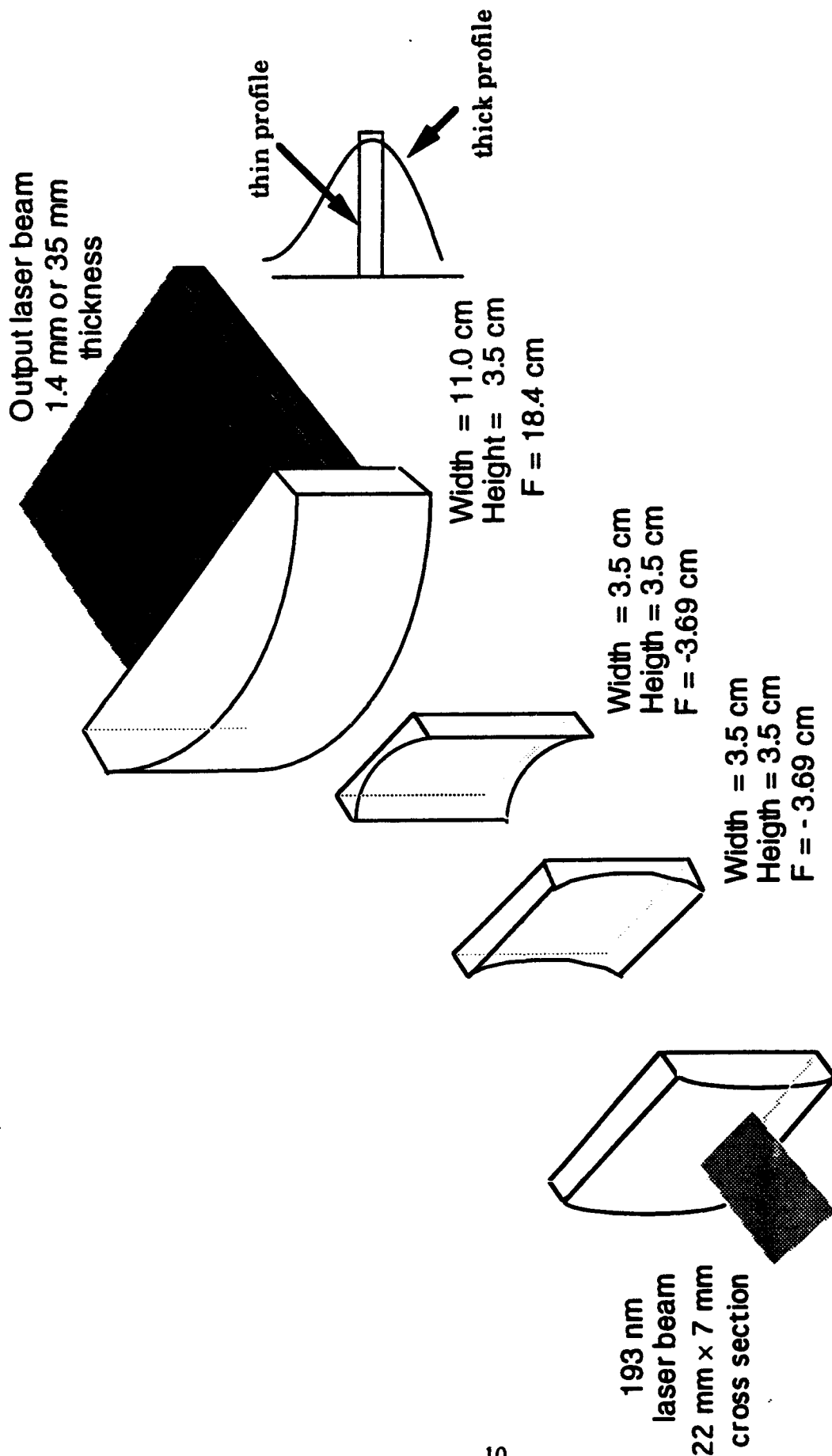


Fig. 3. XUV laser optical beam forming system.

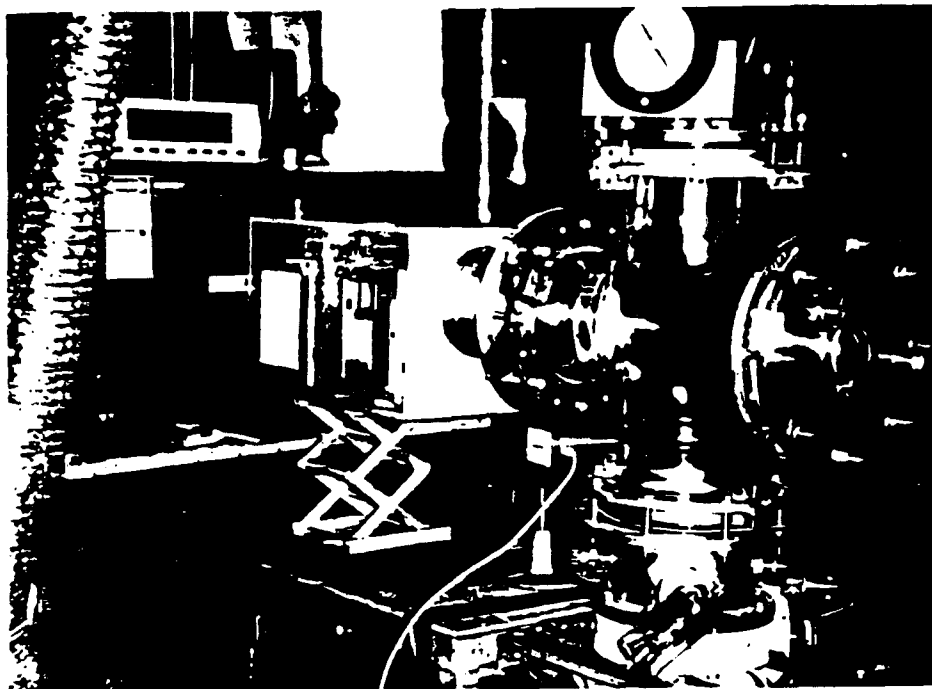


Fig. 4. XUV Laser Sheet Beam Experimental Facility.

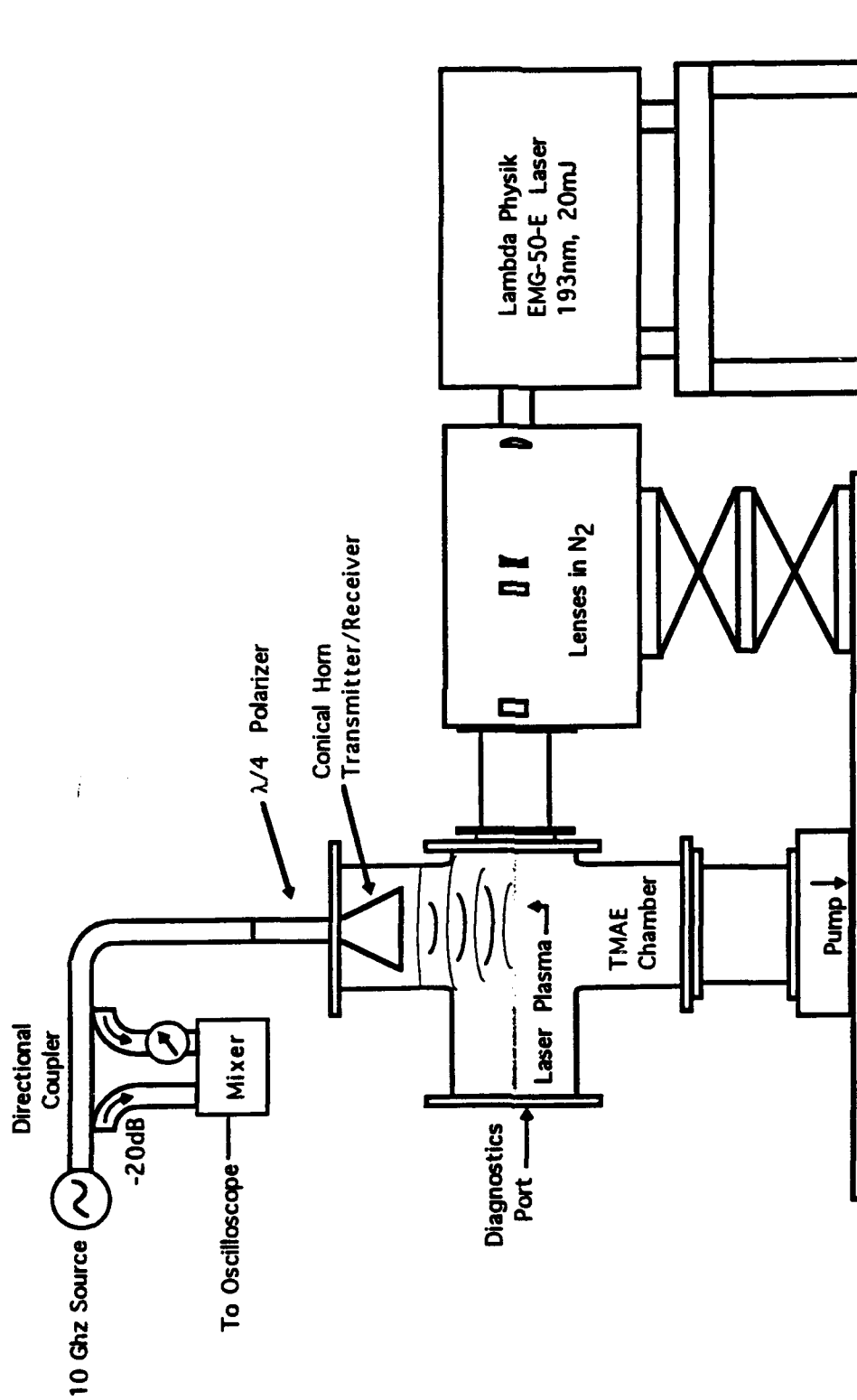


Fig. 5. Laser Plasma Experimental Facility.

Date: Apr-06-1994

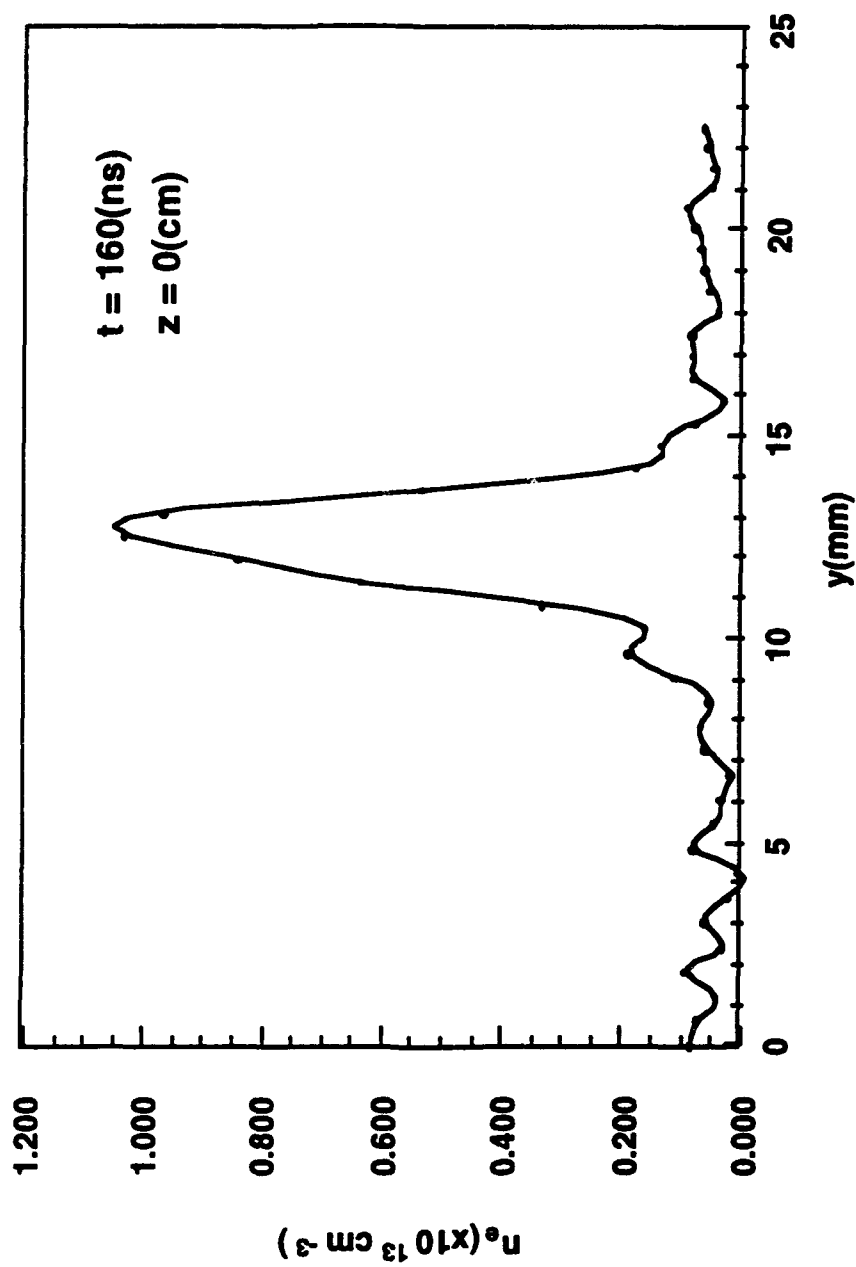


Fig. 6. Plasma transverse profile.

pressure of TMAE is high (500 mT). Figure 6 clearly demonstrates that the plasma density has "sheet"-like profile of a few mm thickness. Within the sharp boundaries of the "sheet" there is a high plasma density region. The plasma frequency corresponding to the high density in this region is well above normal microwave frequencies, and the boundary is extremely sharp in the region, thus the plasma sheet can be treated as a total reflection conductor for microwaves in the 10 GHz range.

The peak plasma density at 6-7 cm away from the entrance window decreases to $2.5 \times 10^{12} \text{ cm}^{-3}$ (Fig. 7). This plasma density decay is caused by the strong absorption of the photon energy by the TMAE molecule. At lower neutral filling pressures (100 mT) the decay is slower but the overall plasma density decreases accordingly when the laser power is kept constant. With higher laser power we expect to obtain higher overall density plasma with less longitudinal attenuation.

Besides plasma measurements, we have also made some measurements of our optical system. The qualitative results indicate a very nice compression in Y-direction and expansion in X-direction of the incident laser beam by the lens system. In the Y-direction (vertically), the compression factor is about 3-5, close to the design value. In the X-direction (horizontally), the width of the output laser beam is > 10 cm compared with 2.2 cm for the input. Precision beam profile mapping will be carried out by a new photo-diode detection system.

Measurements on the x-y plane are being made with two Hamamatsu UV-sensitive photodiodes. One will be kept stationary as a reference, since the laser intensity varies from shot to shot. The other will be moved in the x-y plane. These measurements will be made before the laser beam enters the plasma chamber. Each diode surface has a 1.1 mm square dimension. The mobile one will be moved in increments as small as 0.1 mm in the x-y plane.

The laser beam decay in the z-direction (direction of propagation) provides a cross check for the plasma density and temperature measurements. This will be accomplished by assuming that any photon that enters the TMAE gas either ionizes a molecule or heats a free electron. Laser intensity measurements in the z-direction will be made simultaneously with the plasma density and temperature

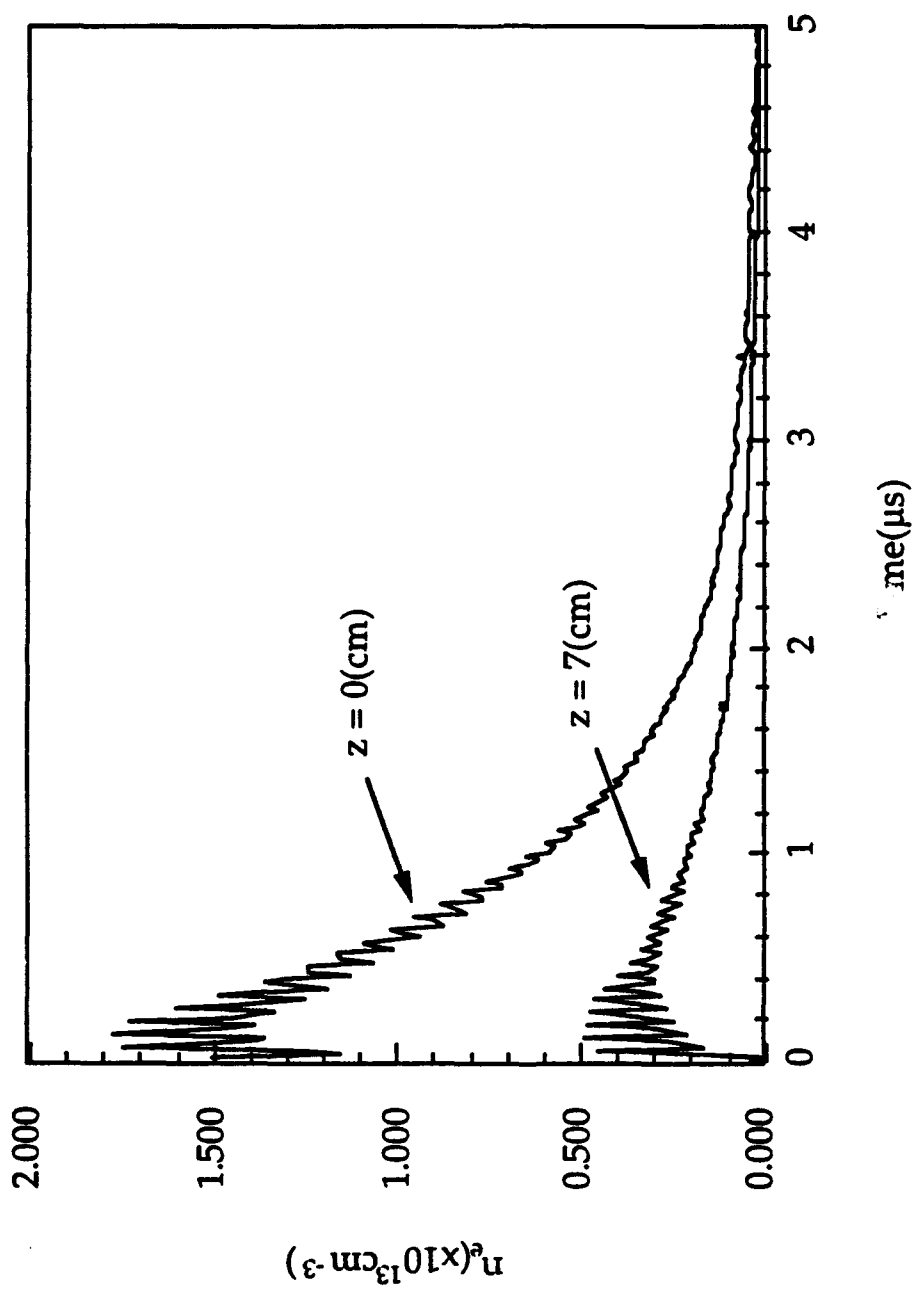


Fig. 7 Plasma density vs. time at two positions along the beam.

measurements. One photodiode will remain stationary as a reference while the other is moved in the z-direction inside the plasma chamber.

A third cross check on Langmuir probe density and temperature measurements is progress. A triple probe¹¹ has been constructed to measure the time dependence of the plasma density and temperature in space.

We are also designing a 10 GHz narrow beam conical horn to test the properties of the plasma mirror. The beamwidth of 3-5 degrees is desirable to obtain a localized reflection for the backscattered microwaves. A narrow beamwidth provides less variation in plasma density over the beamwidth. To obtain such a narrow beamwidth we plan to include corrugations in the horn and a dielectric. Figure 5 illustrates the overall system.

b) Data analysis and modeling

The existence of such a "sheet" plasma is the result of an initial photo-ionization and the subsequent complex physical processes of diffusion, recombination and attachment.

We have also made a calculation of microwave reflection coefficient at normal incidence upon high density plasma. The model uses well-known Epstein profile and simple collisional model. Physically, the parameters which determine such a profile are: plasma thickness, peak density, collision frequency. We calculated the reflection and absorption coefficients for two very different profiles. Using a sharp boundary model, the reflection coefficient was estimated to be 99% for a 10 GHz wave. On the other hand, when a diffuse profile is used, the plasma becomes absorptive and the absorption coefficient is > 75% for 10 GHz and 99.5% for 30 GHz waves.

We have begun a detailed data analysis of the measurements of transverse plasma density (in the presence of the lens system). Measurements of the transverse distribution of the plasma show that peak density of the order of $1.0 \times 10^{13} \text{ cm}^{-3}$ can be obtained. This plasma is now being experimentally characterized. After the end of the laser pulse, the behavior of the plasma density is determined by the equation

$$\frac{\partial n}{\partial t} = D \frac{\partial^2 n}{\partial y^2} - \alpha n - \beta n^2,$$

where D = diffusion coefficient, α = electron-neutral collision frequency, β = electron - ion recombination rate. For a short period after the end of the laser pulse (~ 100 ns), both diffusion and recombination occur near the axis. However, for distances far away from the axis, we expect diffusion to dominate. The diffusion equation can be solved analytically for $n(y,t)$, given an initial plasma profile $n(y,0)$. Assuming an initial Gaussian profile $n(y,0) = n_0 \exp(-y^2/a^2)$, it turns out $n(y,t)$ is actually another Gaussian with a time-dependent width. Explicitly,

$$n(y,t) = n_0 \frac{a}{\sqrt{4Dt + a^2}} \exp\left[-\frac{y^2}{4Dt + a^2}\right]$$

In Fig. 8, we show a plot of measured $n(y,t)$ vs. y^2 for y in the 0.4 - 1.0 cm range, at $t = 100$ ns. At least squares fit to the data yields gives a formula for D as $1/(4Dt + a^2) = 0.84 \text{ cm}^{-2}$. With $t = 100$ ns and the laser beam with a estimated as 2 mm, we obtain $D \sim 2.9 \times 10^6 \text{ cm}^2/\text{s}$. It should be noted, however, that this can only be considered as an estimate of D since for the values of y and t considered in these experiments, the magnitude of the diffusion term $D \frac{\partial^2 n}{\partial y^2}$ may still be comparable to that of the recombination term βn^2 (recall that $\beta = 1.8 \times 10^{-6} \text{ cm}^3/\text{s}$ from data at later times $t \sim 1 \mu\text{s}$). Specifically, with D in the $10^5 - 10^6 \text{ cm}^2/\text{s}$ range, we found that the ratio of diffusion over combination rates can be in the 1 - 10 range. We plan measurements at larger distances from the axis, where diffusion can be expected to dominate recombination.

Our work has been presented as a poster at the 35th Annual meeting, APS DPP, Nov. 1993 at St. Louis, MO. The title is "XUV Laser Produced Plasma Sheet Beam and Microwave Agile Mirror" by W. Shen, Y.S. Zhang, J.E. Scharer and N.T. Lam.

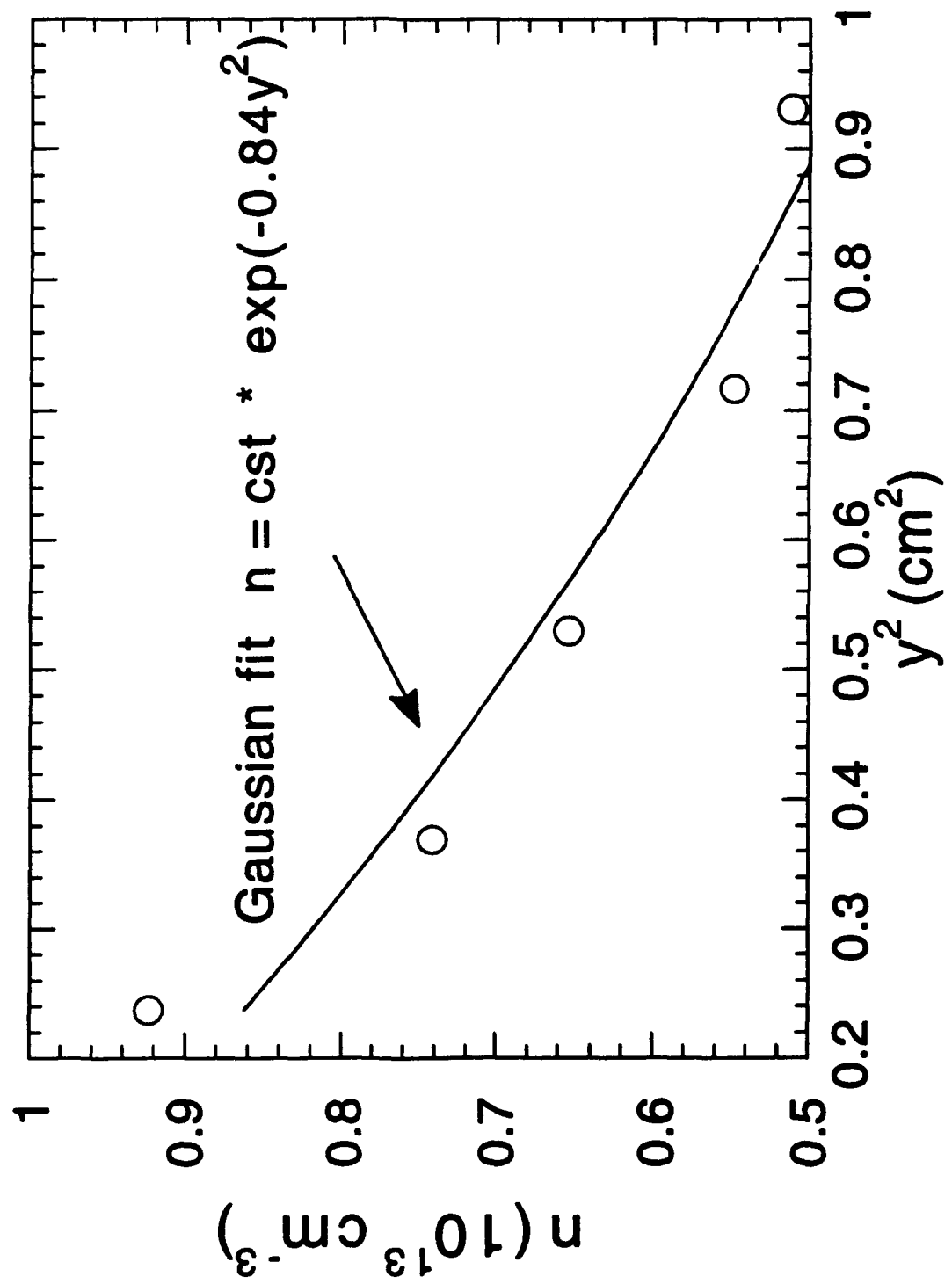


Fig. 8. Plasma transverse profile.

B. Broadband Transmission and Backscatter Measurements in a Cyclotron Resonant Plasma

B.1. Network Analyzer and Homodyne Backscatter Measurements

We have made substantial progress on measurements and analysis of broadband microwave absorption and transmission between two antennas as well as antenna backscatter observations in a cyclotron resonant plasma. The experimental facility is shown in Fig. 9. This research has been described in a paper¹ which has recently been published.

We have developed a homodyne detection system that is capable of detecting the scattering targets in a noisy plasma environment at very low scattered power levels. The system uses a lock-in voltmeter (basically a cross correlator) to detect the scattered signal in the high noise plasma background. The improvements include: incorporation of a modulating PIN diode in the ceramic coated dipole antenna and studies of the effects of a greater variation in the modulating frequency (from 10 kHz to 1 MHz) to both PIN diode dipole antennas and bare tantalum disc Langmuir probes.

We have investigated the propagation, broadband absorption and scattering of electron cyclotron waves from a dipole antenna in an inhomogeneous plasma. The use of network analyzer and homodyne modulated scatterer techniques have allowed more detailed results to be obtained which describe the properties of waves launched in an inhomogeneous, warm plasma and their transmission between and backscattering from dipole and helical antennas. The use of direct transmission between the helical antenna launcher and a receiving dipole located 1.1 m apart shows that -50 dB attenuation of the signal for plasma densities of $3 \times 10^{11} \text{ cm}^{-3}$ and temperatures of 4 eV can be obtained through the cyclotron resonance. This is comparable to the integral of the hot plasma damping decrement through the resonance zone with negligible collisional effects.

The network analyzer results presented in Fig. 10 shows that transmission losses of 40-50 dB occur when a cyclotron resonance is located between the helical antenna launcher and dipole antenna receiver. This can be obtained over a frequency range of 1.5-3.0 GHz for the plasma parameters observed in the

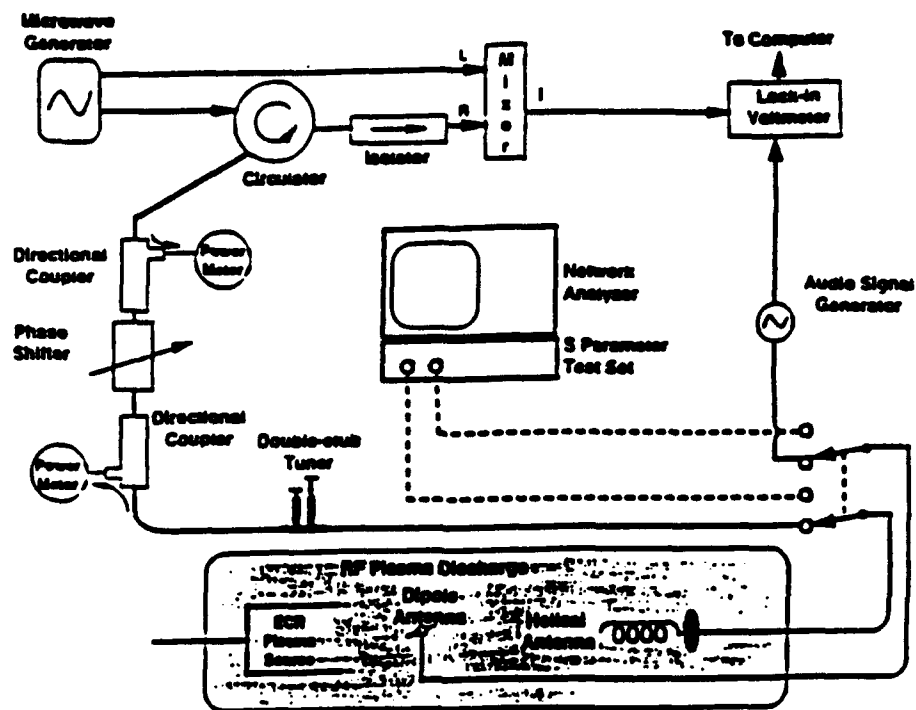


Fig. 9. Microwave plasma facility for propagation, absorption and backscatter studies.

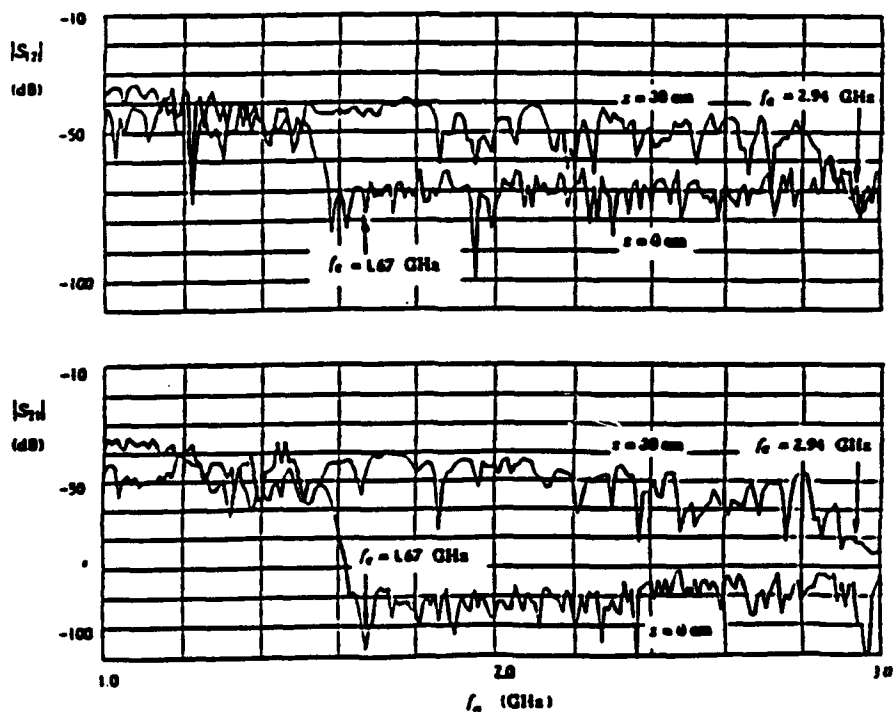


Fig. 10. Broadband network analyzer transmission traces between two antennas at two dipole locations.

inhomogeneous magnetic field. The results show a Doppler shifted absorption which starts at $f/f_c=0.92-0.94$ which is slightly before that predicted by WKB hot plasma cyclotron damping and in closer agreement with a full wave kinetic theory.⁷ It is concluded that the plasma column and helical antenna launch parameters admit only very pure (- 40 dB) right-hand polarized modes to be received by the dipole antenna.

The two antenna system shows a non-reciprocal behavior at higher densities due to the hot plasma. The difference in the two directions for transmission signals at frequencies where absorption and evanescence zones exist between the two antennas is 20 dB at higher plasma densities and is reduced as the plasma density is decreased. It is argued that this is due to the difference in launched power characteristics for the two antennas and the consequent mode conversion for evanescent waves in a hot, anisotropic plasma as wave power propagates between them.

The modulated scatterer and homodyne system is used to determine the microwave backscatter from a given region of the plasma where all other reflections in a finite plasma column are suppressed. Reductions in the backscatter of 40 dB are observed due to the presence of a cyclotron resonance zone between the two antennas. Figure 11 illustrates the 1.9 GHz backscatter signal received by the helix as a dipole antenna is moved through the cyclotron resonance zone at 7 cm. This compares with 30 dB microwave backscatter reductions observed by Destler et al.⁸ for pulsed plasmas produced by coaxial guns in the absence of a magnetic field. Backscatter wavelengths half the local hot plasma cyclotron wavelength are also observed for our case. Fast Fourier transform analysis of the real part of the backscatter signal is shown to agree well with quasi-parallel propagation hot plasma theoretical predictions for local wave numbers. This method is shown to be sensitive over a 70 dB dynamic range and down to launched power levels of -70 dBm. Ray tracing results in an inhomogeneous plasma column indicate quasi-parallel energy flow near the center of the plasma column. In addition, a vacuum boundary analysis of a plasma column and use of the ANTENA code is shown to yield quasi-parallel ($k_z \gg k_\perp$) propagation for electron cyclotron waves near cyclotron resonance ($f/f_{ce} \approx 0.9$) for our plasma parameters.

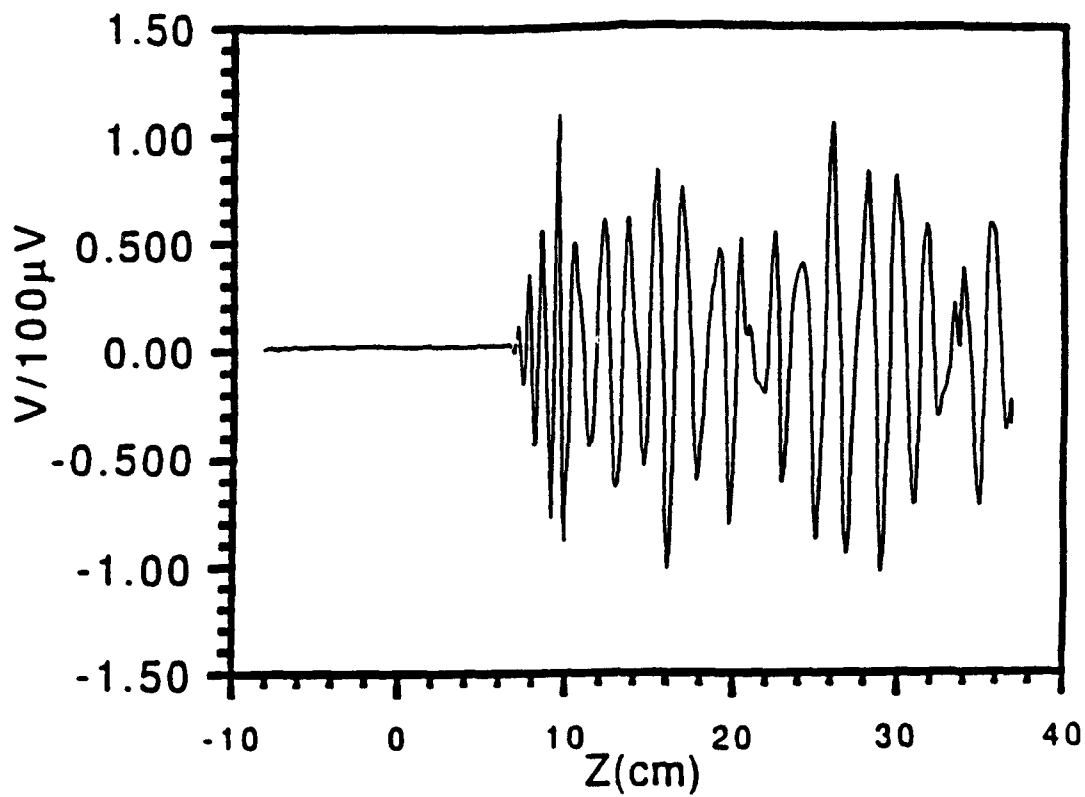


Fig. 11. Dipole backscatter signal at $f = 1.9$ GHz.

In order to simulate the propagation of a right-polarized wave excited by an antenna in a laboratory plasma of finite size, we have used the code ANTENA: a code which calculates the wave fields in a cylindrical plasma imposed by an external coil structure (B. McVey, MIT report PFC/RR-84-12, 1984). In particular, ANTENA allows us to isolate a mode with a particular azimuthal number and calculate its spectrum, polarization and power flow characteristics in the plasma. We have chosen plasma and coil parameters which are appropriate for a typical backscattering experiment : $n_e = 3 \times 10^{11} \text{ cm}^{-3}$; $B_0 = 800 \text{ G}$; $f = 2 \text{ GHz}$; cylinder radius $a = 6 \text{ cm}$. For simplicity, the plasma density has been assumed uniform and the coil taken as a short Nagoya type III coil. We have carried out ANTENA runs to determine the propagation characteristics of the mode with azimuthal number $m = 1$ (which has a polarization appropriate for resonance with the electrons). The results show that quasi-parallel propagation (in the sense that $k_{\perp} \ll k_{\parallel}$) of the electron cyclotron wave near the axis is possible in a plasma of laboratory size.

Quantitative analysis of the broadband network analyzer transmission and backscatter measurements were carried out. The theoretical values of k_r and k_i are derived from a numerical solution of the WKB hot plasma dispersion relation, for typical values of density and temperature ($n_e = 3 \times 10^{11} \text{ cm}^{-3}$ and $T_e = 3.5 \text{ eV}$). We find good agreement between theory and experiment, as far as k_r is concerned. In general, the experimental k_i vs. f/f_c curve lies above the theoretical curve, with the greatest deviation occurring near f_c . Near the position of cyclotron resonance, the measured damping decrement increases above that predicted by local WKB hot plasma collisionless damping, in agreement with the strong damping predicted by Fruchtman et al.⁷ This regime of strong magnetic gradients is also of interest in the area of plasma sources for materials processing.

We have modified our experiment so that we can measure the 3-D fields of an electron cyclotron launched by a helical antenna and wave propagating into a magnetic beach. Measurements are made with three orthogonal coils which measure the local magnetic flux's time rate of change. The modifications required 1) the design and construction of suitable coils, 2) Developing a suitable detection system, 3) interfacing with the computer and developing appropriate software for Labview, and 4) the development of new analysis tools to aid in interpreting the data.

B.2. Coil Design for 3-D Microwave Field Measurements

Coil design is especially challenging in our experiment. To avoid cross talk between measured fields we must use shielded coaxial lines. This unavoidably increases the bulk of the measuring device which becomes a fairly significant scatterer for the electron cyclotron wave. Perhaps more significant is the requirement that the coil's circumference be less than $\lambda/10$ to accurately measure wave amplitude and phase. The flux area of the coils is then correspondingly small, decreasing the sensitivity of the probe. As the wave approaches resonance the wavelength becomes quite small (around 2 cm). The loops should ideally have a circumference of around 2 mm.

The loops are made using the inner conductor wire of a 0.037" semi-rigid coaxial cable. The inner conductor has a diameter of 0.011" and is wrapped around a .025" diameter core (corresponding to an inner circumference of approximately 4 mm). To increase the sensitivity of the detector five loops are made giving the coil an axial length of approximately .070" (Fig. 12). The loops are then coated with an insulating material to reduce the direct electro-static contact with the plasma. The three loops are rigidly connected and rotated through the plasma cross section (Fig. 13) and scanned axially.

B.3. Detection Scheme

The launched electron cyclotron wave is amplitude modulated with a low frequency (10-100 kHz) signal. The signals detected with the coils are down shifted using a mixer with the local oscillator driven at the 2 GHz microwave frequency and detected using lock-in voltmeters referenced at the modulation frequency. These measurements yield both amplitude and phase information and filter out signals introduced by the system sufficiently far removed from the modulation frequency. This detection scheme requires that the modulation frequency and amplitude be higher or of larger amplitude than the low frequency turbulence present in our system. Current efforts are aimed at improving the sensitivity of the detection system at sufficiently high frequencies and amplitudes.

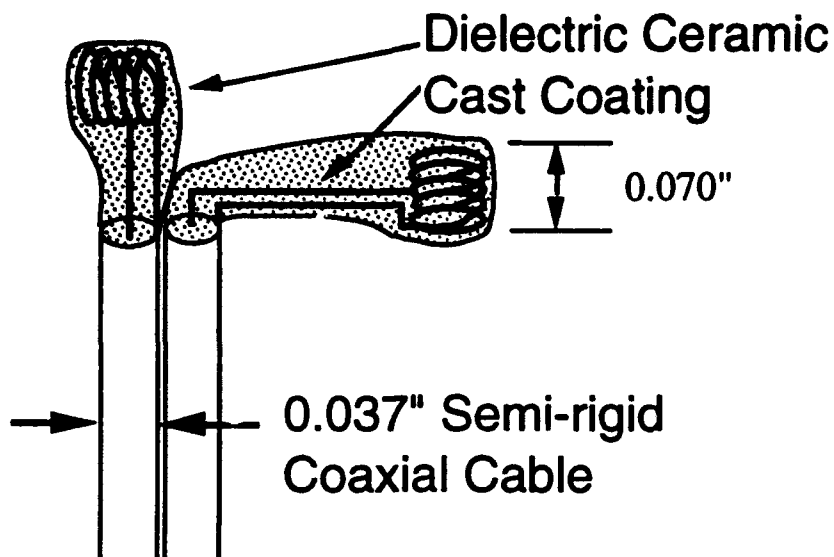


Figure 12. Representation of two orthogonal loops used to measure the magnetic fields. Outer diameter of the coaxial cables is .037" while the inner conductor has a diameter of 0.011".

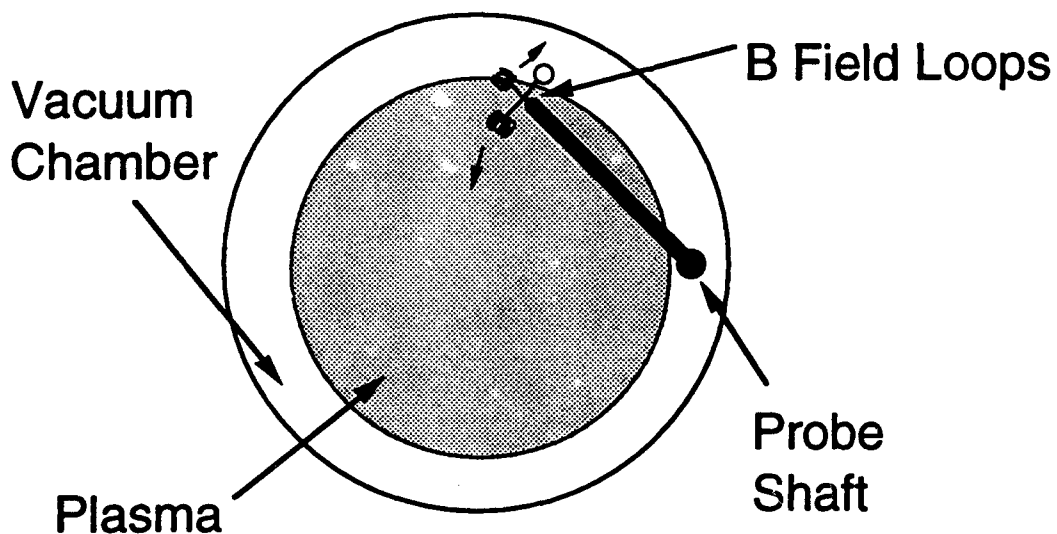


Figure 13. Schematic of Measuring system. Three orthogonal loops are located at end of probe which is rotated through the plasma around the probe shaft. The probe shaft is electronically driven to sample the fields at various axial positions. Probe dimensions are exaggerated for visualization.

B.4. Computer Interfacing and Software Development

The data acquisition system used previously was based on an IBM AT system. The software available did not readily lend itself to the necessary acquisition and analysis functions for the 3-D field measurements. Therefore, it has been necessary to switch to the Macintosh based Labview software package. A new interfacing circuit had to be built and Labview virtual instruments for acquiring, analyzing, and storing the data had to be developed. The detection system reads each field value sequentially and records the spatial position of the coils and the operating conditions when the sample is taken.

B.5. Analysis and MAGIC Computer Simulation

The general analytic analysis of wave propagation in a strongly inhomogeneous plasma is quite complex. The inhomogeneity in the plasma parameters coupled with the boundary conditions for the helix and the waveguide make traditional electromagnetic approaches to radiation, propagation, and scattering problems untenable. To aid in our understanding of our experimental results and to further clarify the basic physical issues present, we have begun a numerical simulation of the experiment using the particle-in-the-cell (PIC) code MAGIC, developed by Mission Research Corporation (MRC).

The PIC code has several advantages for analyzing problems similar to ours. First, the codes readily accounts for arbitrary boundary surfaces and inhomogeneities in the electromagnetic medium. Thus we can simulate systems in which the system parameters closely approximate the measured plasma parameters (e.g. density profiles, temperature profiles) in our experiment.

Unfortunately, there are also several relevant difficulties inherent in PIC codes. First, the simulation must use a macro particle representing a large collection of physical particles. When the macro-particles become too large (i.e. represent too many individual particles) the physical picture suffers. For instance, the charge separation which occurs randomly in the plasma is greatly exaggerated in the simulation, resulting in artificially high electrostatic fields self-induced by the plasma (so called stochastic heating). To observe the desired electric fields the power level must be increased artificially high so that the wave effects can be distinguished

from the stochastic effects yet keeping the plasma response linear. Another difficulty is that the stochastic fields result in plasma self heating, thus making it difficult to control the plasma temperature.

We have benefited from the help of Dr. Larry Ludeking and Dr. Dave Smythe at MRC. Dr. Ludeking conducted a four day seminar in Madison introducing us to the logistics of the code and helped in getting our simulations started. Dr. Smythe, who has done previous simulations on electron cyclotron heating and also developed the helix model used, has given suggestions that helped us in understanding some of the basic issues associated with the code. However, we are using MAGIC to simulate a plasma regime not previously examined with the code. Determining the correct simulation parameters for our experiment is a topic which is still being carried out.

The simulation uses plasma densities of the order 10^{11} cm^{-3} and magnetic field strengths corresponding to ω/ω_{ce} of roughly 1.5 at the helix's center ($z=50 \text{ cm}$) to a resonance at $z=10 \text{ cm}$. The helix is taken to have a pitch angle of 13° with a radius of 1.1 cm and is immersed in the center of the plasma. The helix should excite a dominantly RHCP wave. However, as stated above the helix model has been difficult to use and we have found that a current loop oriented perpendicular to the magnetic field direction tends to be the best exciter.

To date we have carried out MAGIC simulations for both uniform and experimentally measured density profiles. We have found it advantageous to observe the magnetic fields rather than the electric fields, since the electrostatic fields excited in the simulation swamp out the electromagnetic component of the E fields (Fig. 14). As shown in Fig. 15 the simulated magnetic fields show many of the same characteristics as our backscatter results, namely damping at the Doppler broadened resonance zone, an increasing but finite wavenumber as the wave approaches the resonance, and amplitude modulations.

Once the determination of basic simulation parameters has been achieved, we will use MAGIC to address issues specific to our experiment, such as scattering from conducting and dielectric objects in the anisotropic plasma, and the wave guiding effects of the hollow density profile predicted by ray tracing. A poster summarizing this work, "Electron Cyclotron Waves in a Highly Inhomogeneous Plasma," by

MAGIC VERSION APRIL 1993 DATE Sep 13 1993
 SIMULATION Dipole in a Magnetic Beach version 66

PLOT AT TIME 1.25E-08 SEC
 E2 COMPONENT
 RANGING FROM (19,7) TO (124,7)

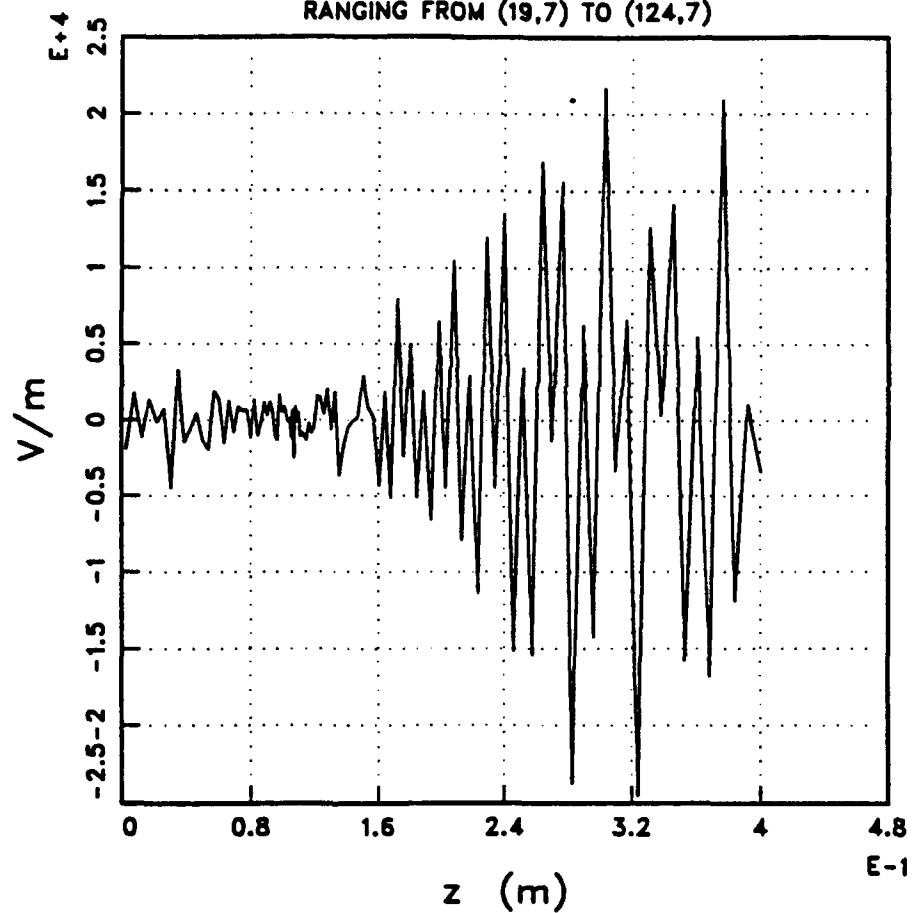


Fig. 14. MAGIC simulation of E_z in a magnetic beach. Short wavelength electrostatic fields are superimposed on the longer wavelength electromagnetic mode.

MAGIC VERSION APRIL 1993 DATE Sep 13 1993
SIMULATION Dipole in a Magnetic Beach version 67

PLOT AT TIME 1.50E-08 SEC
B1 COMPONENT
RANGING FROM (19,7) TO (124,7)

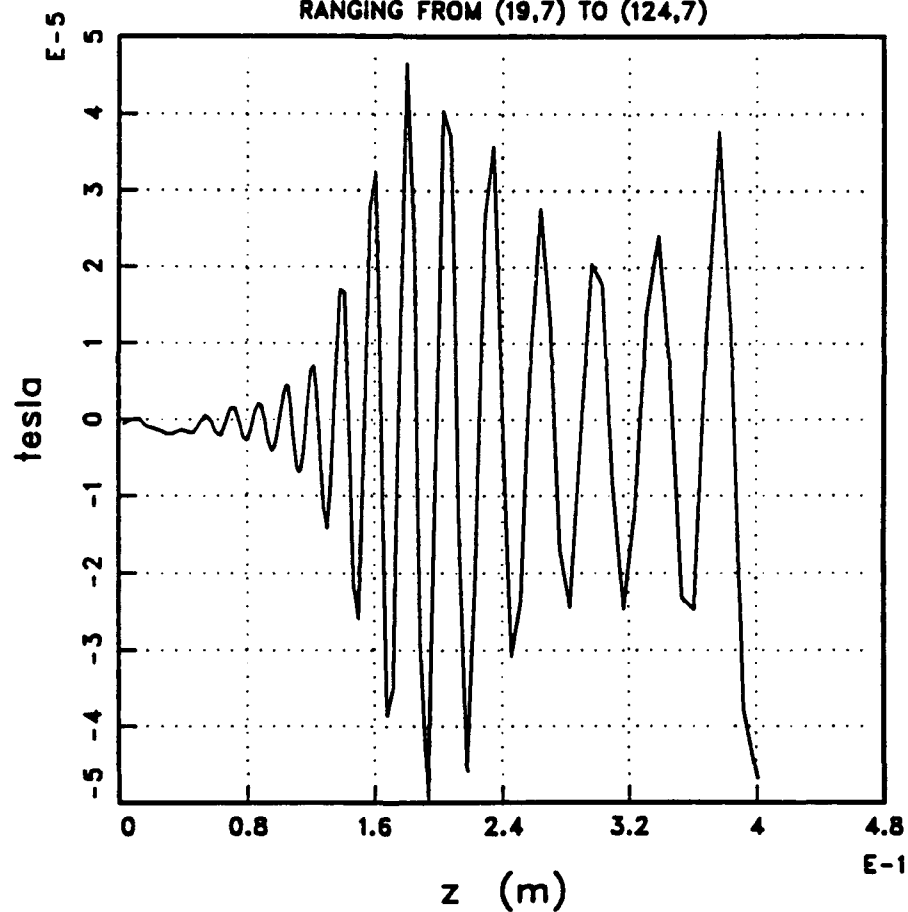


Fig. 15. The B_z field for an electron cyclotron wave in a magnetic beach.

Brian E. Chapman, John E. Scharer, Yong-Shan Zhang, and Weimin Shen has been presented at the APS Plasma Physics Conference, St. Louis, MO, Nov. 1-5, 1993.

C. Electron Cyclotron Wave Scattering by a Probe-Launched Ion Acoustic Wave

We have continued our measurements of backscattered signals from an encapsulated diode loaded dipole. We have been able to make measurements showing highly repeatable phase and amplitude information. The measurements show that as the modulating frequency increases a decrease in the backscattered signal level is obtained for cases when the scatter is located behind the spatial region for electron cyclotron resonance in the magnetic beach.

We have demonstrated that the encapsulated dipole can excite ion acoustic waves. We have observed the ion acoustic waves in the frequency range of 500 kHz to 1.5 MHz. The optimum excitation occurs at around 900 kHz. The raw and filtered signals using our Labview data acquisition system are shown in Figs. 16a) and 16b). The ion acoustic waves are highly damped due to collisions and are not observable after about 5 wavelengths.

We have recently examined the influence of the scattering antenna launched ion acoustic waves caused by the modulation frequency on the backscattered microwave signal. The theoretical problem of electromagnetic wave scattering in a plasma half-space with a propagating density perturbation and a transverse conducting boundary condition was considered. An analytical solution of the scattered wave field was obtained from a one-dimensional model. The results show that there are two different types of scattered waves. One propagates only in the region where the plasma density is perturbed; its frequency and wave vector satisfy the conditions for a three wave interaction process. The other propagates as an unperturbed electron cyclotron mode with the frequency up- or down-shifted.

Experiments were performed to examine electron cyclotron wave scattering by an ion-acoustic wave excited by means of a grid along the magnetic field line in a mirror machine. The density perturbation and wavelength of the ion-acoustic wave were measured. A right-hand circularly-polarized electron cyclotron wave is launched by means of a helix antenna from one end of the mirror. The backscattered waves propagating away from the density perturbation region are

Ion Acoustic Wave Signal

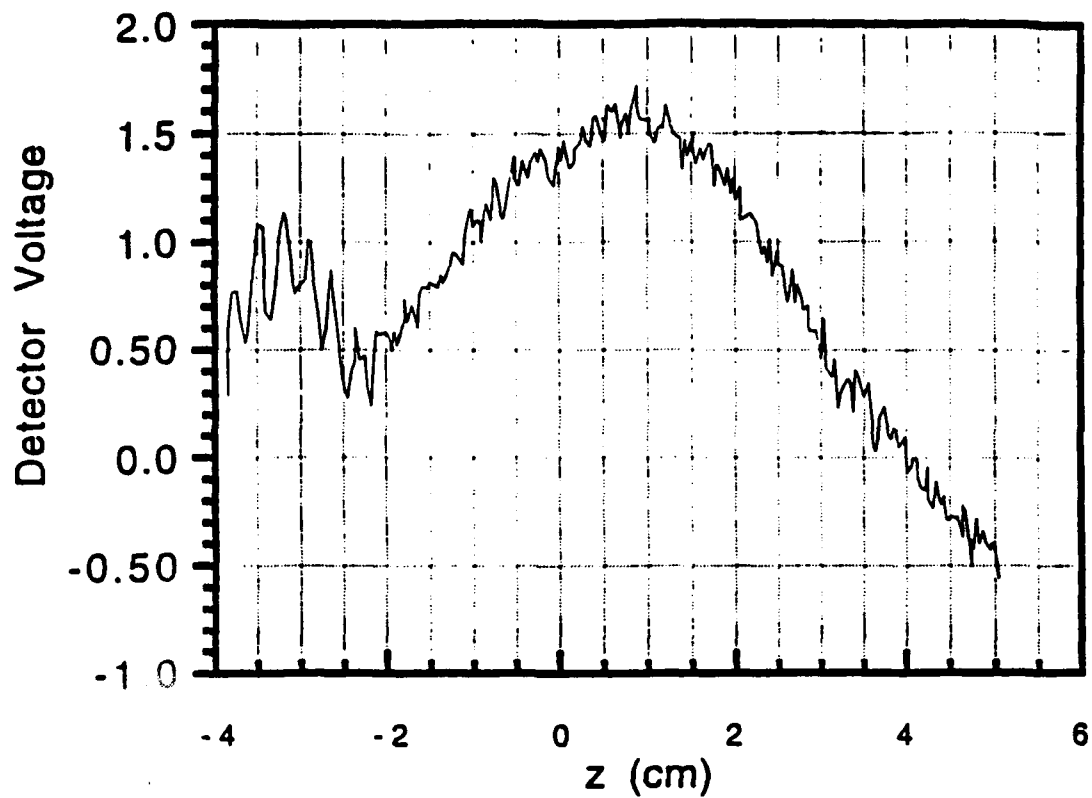


Fig. 16a. Unfiltered ion acoustic wave signal.

Ion Acoustic Wave Filtered Signal

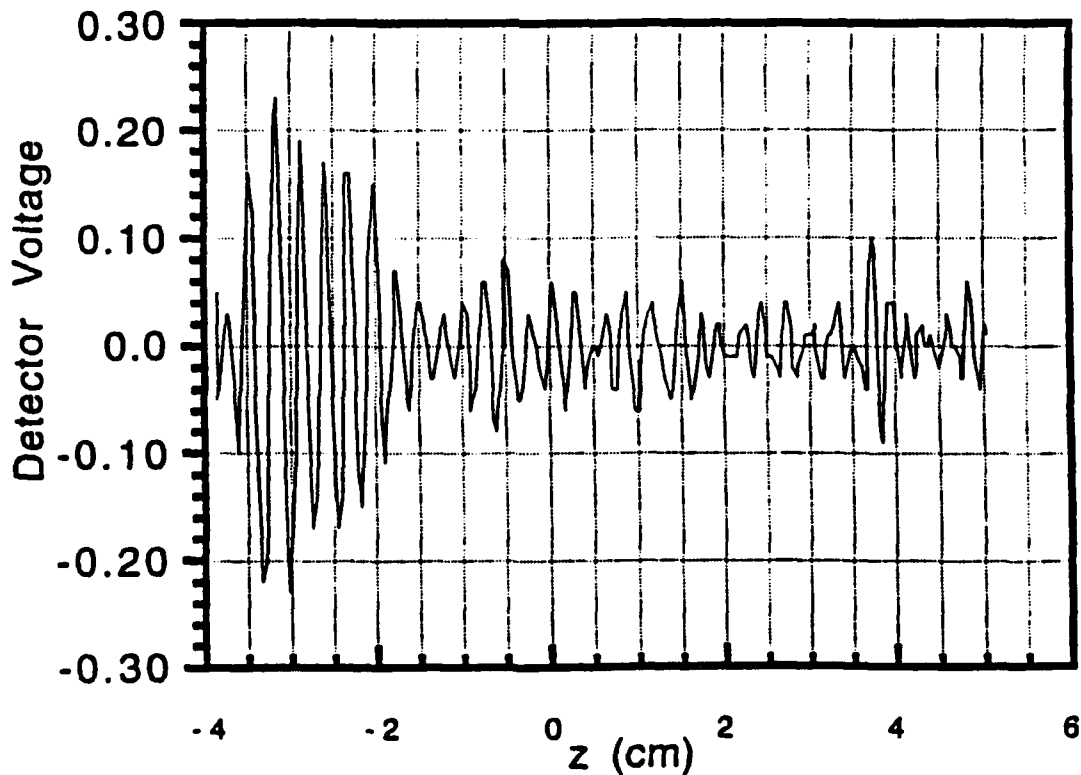


Fig. 16b. Ion acoustic wave signal after passing through a bandpass filter.

measured, and their dependence on the ion-acoustic wavelength was examined. The scattered wave inside the region where the ion-acoustic wave propagates is examined by measuring the scattered wave field pattern when the ion acoustic wave number is much larger than that of the incident wave. The experimental results are shown to agree very well with theory. This research has been written as a report and published in the Physics of Fluids.⁹

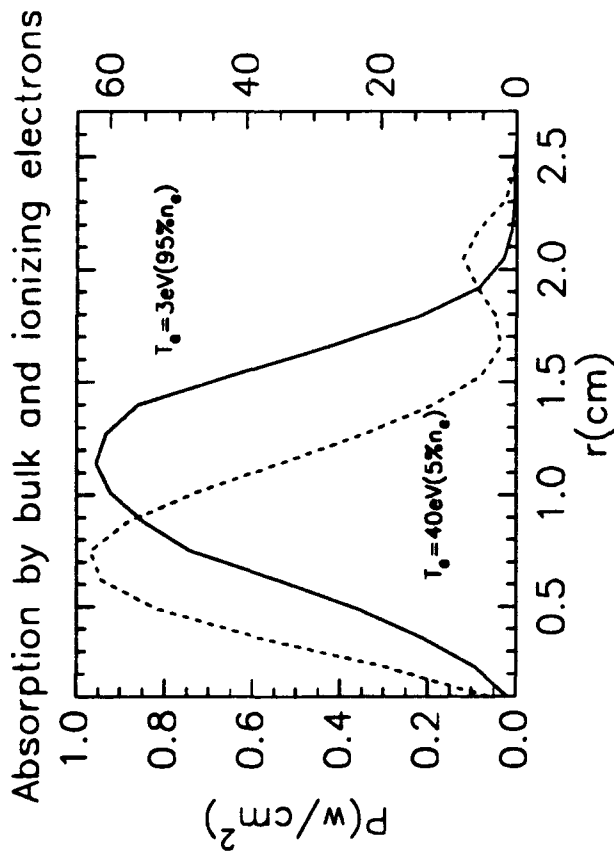
D. RF Plasma Source Computer Code

We have made improvements in the ANTENA code [10] that computes the 3-D electromagnetic fields in a cylindrical hot magnetized plasma surrounded by an RF inductive coil, both of which are enclosed in a metal conducting tube. The original application of the ANTENA code was to study ion cyclotron heating of magnetic fusion plasmas. We have generalized the code to examine radiofrequency sources for the production of high density plasmas ($n_e \approx 10^{13} \text{ cm}^{-3}$). We have ported the code from CRAY facilities to our UNIX-based workstations (typically run on IBM RS/6000s), using the free software graphics package PLPLOT. We increased the radial mesh size (up to 1600 radial points) for the stratified plasma density and temperature profiles, to accommodate all ranges of frequencies from the ion cyclotron frequency to the electron cyclotron frequency. This allows us to study and model high density plasma sources. We have also upgraded the code to include helical coils. In particular, we have studied plasma density and temperature profile effects on power absorption of small fraction ($n_{fe}/n_e \approx 5\%$) ionizing fast electrons ($T_e = 40\text{eV}$) and bulk ($T_e = 3\text{eV}$) electron distributions in the model.

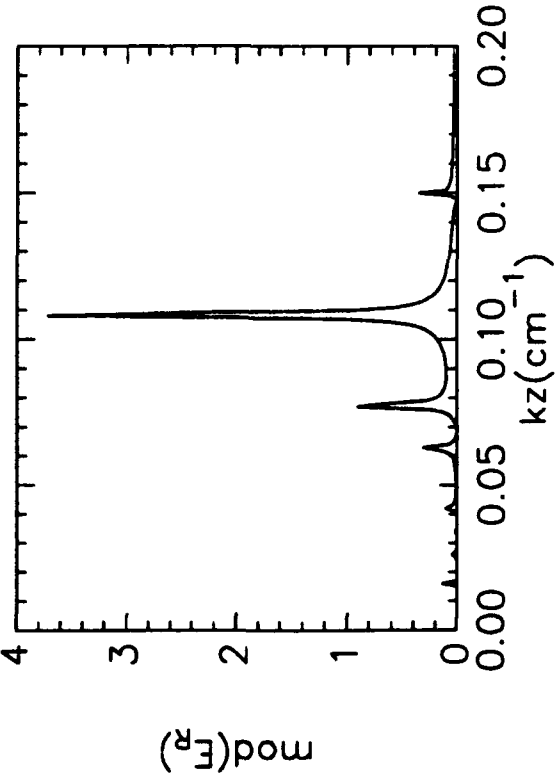
Figure 17 illustrates the radial power absorbed by the bulk and fast ionizing electrons, and also the kz -spectrum at the plasma radius shown, for the Nagoya type III and the partial turn helical coil used in our model. These results were taken for a parabolic density and temperature profile of 2.5 cm plasma radius, using argon gas and an applied RF power of 800 Watts at a frequency of $f = 8 \text{ MHz}$. The solid and dashed curves correspond respectively to the left-hand and right-hand scale. Collisional effects are not included. The fractional helix could excite either the $m = +1$ or $m = -1$ azimuthal mode corresponding to coil rotation.

The results show that this type of antenna heats the plasma more efficiently than the Nagoya type III coil and produces a broad ($m = +1$) high density

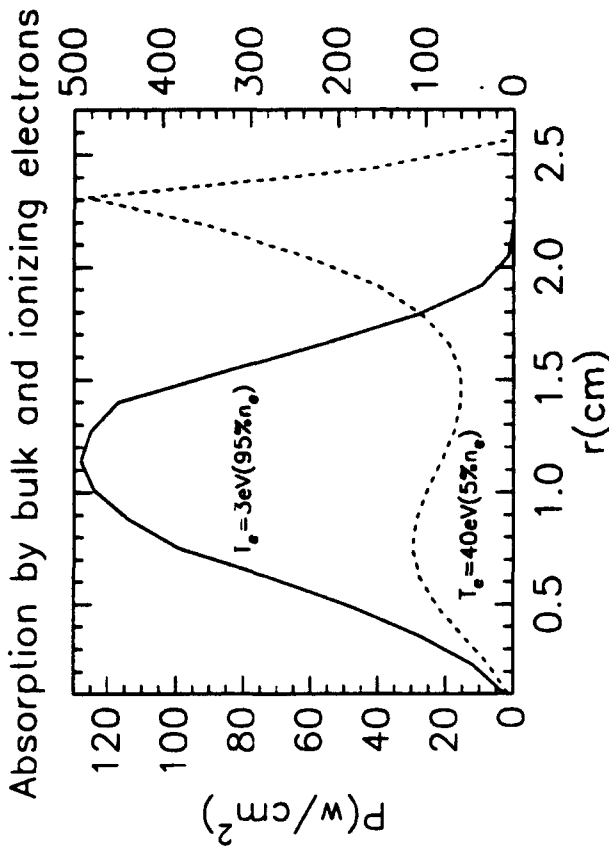
Nagoya type III coil



kz -spectrum of Nagoya type III coil
at $r=0.5\text{ cm}$



Fractional helix coil



kz -spectrum of fractional helix coil
at $r=0.8\text{ cm}$

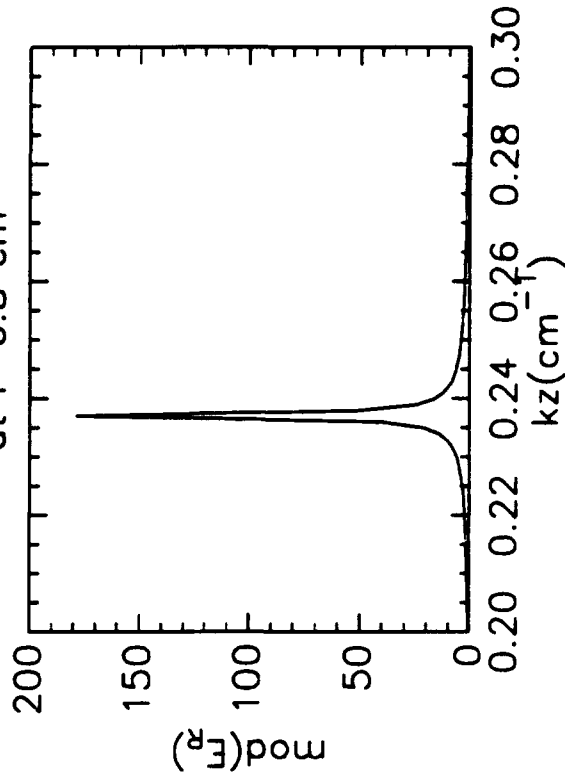


Fig. 17. RF Plasma Source power absorption and k_z spectrum.

($n_e = 2 \times 10^{13} \text{ cm}^{-3}$) plasma. This dominant $m = +1$ mode which is right-hand polarized, heats the plasma near the center. The model also shows that the power absorbed by the plasma is due to Landau damping of the wave. This is shown in Fig. 17 where the kz -spectrum, at the given radial position, peaks at about $\omega/k_z v_{th} = \sqrt{2}$, where the Landau damping rate maximizes. The Krook model used in the ANTENA code to describe collisions shows that the collisional damping of the wave is significant at high densities. We plan to continue to improve this code to examine Landau, collisional and stochastic heating processes. We will optimize the design of the coupling coil to produce uniform, high density plasmas.

References

1. J.E. Scharer, O.C. Eldridge, S.F. Chang, Y.S. Zhang, M. Bettenhausen and N.T. Lam, "Electron Cyclotron Wave Propagation, Absorption, and Backscatter Measurements in a Laboratory Plasma," IEEE Trans. on Plasma Sciences, 21, 271-281 (1993).
2. Y.S. Zhang and J.E. Scharer, "Plasma Generation in TMAE Vapor by an Ultraviolet Laser Pulse," Journal Applied Physics, 73 (10), 4779 (1993).
3. R.J. Vidmar, IEEE Transactions on Plasma Science 18, 733 (1990).
4. K.R. Stadler, R.J. Vidmar, and D.J. Eckstrom, J. Appl. Phys. 72 (11), p. 5089, 1 December 1992; K.R. Stadler and D.J. Eckstrom, J. Appl. Phys. 72 (9), 1 November 1992.
5. Wallace M. Manheimer, IEEE Transaction on Plasma Science, Vol. 19, No. 6, p. 1228, December, (1991).
6. S. Chen and T. Sekiguchi, "Instantaneous Direct-Display System of Plasma Parameters by means of Triple Probe," J. App. Phys., vol. 36, 8, (1965).
7. A. Fruchtman, K. Reidel, H. Weitzner, and D. B. Batchelor, "A Kinetic Full Wave Theory of Strong Spatial Damping of Electron Cyclotron Waves in Nearly Parallel Stratified Plasmas," Phys. Fluids, vol. 30, 115 (1987).
8. W.W. Destler, J.E. DeGrange, H.H. Fleishmann, J. Rodgers and Z. Segalov, "Experimental Studies of High-Power Microwave Reflection, Transmission, and Absorption from a Plasma-Covered Plane Conducting Boundary," J. App. Phys., vol. 69, p. 6313, 1991.
9. Y.S. Zhang, J.E. Scharer, and B.E. Chapman, "Electron Cyclotron Wave Scattering by a Probe Launched Ion-acoustic Wave," Physics of Fluids B 5 (11), 3887-3892 (1993).

10. Y. Mouzouris, J.E. Scharer, N.T. Lam, and M. Bettenhausen, "Applications of ANTENA code to TFTR, high density plasma sources, and wave propagation in a nonuniform magnetized plasma," APS 38, 1887 (1993) St. Louis, MO.

IV. Grant Modalities

Since the start of the grant on May 1, 1991, the participants carrying out the research are as follows:

John E. Scharer, Professor
Owen Eldridge, Visiting Professor
Dr. N. Lam, Scientist
Dr. W. Shen, Postdoc
Dr. Y.S. Zhang, Postdoc
M. Bettenhausen, Graduate Student
B. Chapman, Graduate Student
Y. Mouzouris, Graduate Student
B. Porter, Graduate Student

V. Journal Articles and Theses

1. J.E. Scharer, O.C. Eldridge, S.F. Chang, Y.S. Zhang, M. Bettenhausen and N.T. Lam, "Electron Cyclotron Wave Propagation, Absorption, and Backscatter Measurements in a Laboratory Plasma," IEEE Trans. on Plasma Sciences, 21, 271-281 (1993).
2. Y.S. Zhang and J.E. Scharer, "Plasma Generation in TMAE Vapor by an Ultraviolet Laser Pulse," Journal Applied Physics, 73 (10), 4779 (1993).
3. Y.S. Zhang, J.E. Scharer and B. Chapman, "Electron Cyclotron Wave Scattering by a Probe-Launched Ion Acoustic Wave," Physics of Fluids B 5 (11), 3887-3892 (1993).

4. S.F. Chang, J. Scharer and J. Booske, "Wave Dispersion, Growth Rates and Mode Converter Analysis for a Sheet Beam Hybrid Mode Cerenkov Amplifier," IEEE Plasma Sciences 20, 293-304 (1992).
5. Masters theses (2) are being written by Brian Chapman and Yiannikis Mouzouris on experimental measurements of microwave backscatter from a dipole or Langmuir probe in a plasma and on analyses of transmitting, receiving and scattering properties of antennas in a plasma including the use of the MAGIC code. One (1) master's thesis is being written by Brad Porter on the microwave scattering and absorption from the 193 nm excimer laser produced plasma (Agile mirror).

VI. Conferences (5/91 - 4/94)

1. J.E. Scharer, O.C. Eldridge, S.F. Chang, M.H. Bettenhausen and N.T. Lam, "Experiments and Analysis of Wave Absorption and Backscattering in Plasmas," The 18th International Conference on Plasma Science, Williamsburg, VA, June 3-5, 1991. Conference oral paper.
2. J.E. Scharer, O.C. Eldridge, S.F. Chang, Y.S. Zhang, M.H. Bettenhausen, J. Joe and N.T. Lam, "Experiments and Analysis of Wave Absorption and Backscattering in Plasmas," The 33rd APS Meeting, Tampa, FL, November 4-8, 1991. Bull. of American Physical Soc. Volume 36, page 2485 (1991).
3. J.E. Scharer, O.C. Eldridge, S.F. Chang, Y.D. Zhang, M. Bettenhausen and N.T. Lam, "Electron Cyclotron Wave Propagation, Absorption, and Backscatter Measurements in a Laboratory Plasma," UW-CPTC report #91-15.
4. J.E. Scharer, Y.S. Zhang, N.T. Lam, M. Bettenhausen, O.C. Eldridge, S.F. Chang, and J. Joe, "Experiments and Analysis of Wave Absorption and Backscattering in Plasmas," The IEEE Meeting, Tampa, FL, June 1-3, 1992. Conference oral paper.
5. J.E. Scharer, O.C. Eldridge, S.F. Chang, Y.S. Zhang, M.H. Bettenhausen, J. Joe and N.T. Lam, "Experiments and Analysis of Wave Absorption and Backscattering in Plasmas," The 33rd APS Meeting, Tampa, FL, November 4-8, 1992. Bull. of American Physical Soc. Volume 36, page 2485 (1991).

6. J.E. Scharer, O.C. Eldridge, S.F. Chang, Y.D. Zhang, M. Bettenhausen and N.T. Lam, "Electron Cyclotron Wave Propagation, Absorption, and Backscatter Measurements in a Laboratory Plasma," UW-CPTC report #91-15.
7. AFOSR special equipment proposal "UV laser, large UV flashtube facility and new computer data acquisition facility, supplement to AFOSR Grant 89-353B, "Basic Studies in Plasma/Wave Interactions."
8. Y.S. Zhang, and J.E. Scharer, "Plasma Generation in TMAE Vapor by an Ultraviolet Laser Pulse," CPTC Report #92-3.
9. J. Scharer, Y.S. Zhang, N. Lam, M. Bettenhausen, O. Eldridge and B. Chapman, "Experiments and Analysis of Excimer Laser UV Ionization and Microwave Propagation in Plasmas," The 34th APS meeting, Seattle, WA, Bull. of American Physical Society, 37, 1541 (1992).
10. J.E. Scharer, Y.S. Zhang, N.T. Lam, M.H. Bettenhausen, O.C. Eldridge and B. Chapman, "Experiments and Analysis of Excimer Laser UV Ionization and Microwave Propagation in Plasmas," Bull. Am. Phys. Soc. 37, 1541 (1992).
11. Invited Paper in Microwave-Plasma Interactions Session, J.E. Scharer, Y.S. Zhang, B. Chapman and N.T. Lam, "Experiments and Analysis of Backscatter for Microwave Propagation in a Plasma," IEEE Plasma Conference, Vancouver, BC (1993).
12. Y.S. Zhang, J.E. Scharer and N.T. Lam, "Plasma Generation in an Organic Molecular Gas by an Ultraviolet Laser Pulse," IEEE Plasma Conference, Vancouver, BC (1993).
13. Y.S. Zhang, J. Scharer and B. Chapman, "Electron Cyclotron Wave Scattering by a Probe Launched Electrostatic Ion Wave," IEEE Plasma Conference, Vancouver, BC (1993).
14. W. Shen, Y.S. Zhang, J.E. Scharer and N.T. Lam, "XUV Laser Produced Plasma Sheet Beam and Microwave Agile Mirror," presented at the DPP-APS Meeting, St. Louis, MO (Nov. 1993).

15. B.E. Chapman, J.E. Scharer, Y.S. Zhang, W. Shen, "Electron Cyclotron Waves in a Highly Inhomogeneous Plasma," presented at the DPP-APS Meeting, St. Louis, MO (Nov. 1993).
16. Y. Mouzouris, J.E. Scharer, N.T. Lam, and M. Bettenhausen, "Applications of ANTENA code to TFTR, high density plasma sources, and wave propagation in a nonuniform magnetized plasma," presented at the DPP-APS Meeting, St. Louis, MO (Nov. 1993).